Journal of Asian Ceramic Societies

ISSN: (Print) (Online) Journal homepage: www.tandfonline.com/journals/tace20

Electrocatalytic property of Zn-Al layered double hydroxides for CO_2 electrochemical reduction

Noboru Yamaguchi, Ryosuke Nakazato, Keeko Matsumoto, Masako Kakesu, Nataly Carolina Rosero-Navarro, Akira Miura & Kiyoharu Tadanaga

To cite this article: Noboru Yamaguchi, Ryosuke Nakazato, Keeko Matsumoto, Masako Kakesu, Nataly Carolina Rosero-Navarro, Akira Miura & Kiyoharu Tadanaga (2023) Electrocatalytic property of Zn-Al layered double hydroxides for CO_2 electrochemical reduction, Journal of Asian Ceramic Societies, 11:3, 406-411, DOI: 10.1080/21870764.2023.2236441

To link to this article: https://doi.org/10.1080/21870764.2023.2236441

Published online: 18 Jul 2023.

JOURNAL OF ASIAN CERAMIC SOCIETIES
2023, VOL. 11, NO. 3, 406–411
https://doi.org/10.1080/21870764.2023.2236441

THE CERAMIC SOCIETY OF JAPAN
THE KOREAN CERAMIC SOCIETY
Taylor & Francis
Taylor & Francis Group

RESEARCH ARTICLE

OPEN ACCESS Check for updates

Electrocatalytic property of Zn-Al layered double hydroxides for CO_2 electrochemical reduction

Noboru Yamaguchi[a], Ryosuke Nakazato[b], Keeko Matsumoto[b], Masako Kakesu[b], Nataly Carolina Rosero-Navarro[b,c], Akira Miura[b] and Kiyoharu Tadanaga[b]

[a]Graduate School of Chemical Engineering and Sciences, Hokkaido University, Sapporo, Hokkaido, Japan; [b]Faculty of Engineering, Hokkaido University, Sapporo, Hokkaido, Japan; [c]Instituto de Cerámica Y Vidrio, CSIC, Madrid, Spain

ABSTRACT

Electrocatalytic CO_2 reduction reaction (CO_2RR) has attracted considerable attention as a technology to recycle carbon dioxide (CO_2) into raw materials for chemicals using renewable energies. In this study, the electrocatalytic CO_2RR activity of Zn-Al layered double hydroxides (LDHs) was studied. Zn-Al LDHs loaded carbon sheets were prepared, and CO_2 RR was performed using CO_2-saturated $KHCO_3$ electrolyte to confirm the catalytic ability of Zn-Al LDH. Zn-Al LDHs intercalated with CO_3^{2-} anion were synthesized using the mixture of metal nitrates with the different molar ratio of Zn^{2+}/Al^{3+} by the co-precipitation process, whose corresponding products were named as Zn_2Al_1 LDH, Zn_3Al_1 LDH, and Zn_4Al_1 LDH, respectively. Except for Zn_2Al_1 LDH, ZnO was observed to exist as an impurity. The synthesized Zn-Al LDHs exhibited the electrocatalytic CO_2RR activity for CO formation. In the case of the Zn_2Al_1 LDH, the current density of 15 mA cm^{-2} was obtained with 77% selectivity for CO and 94% selectivity for ($CO + H_2$) at − 1.4 V vs. RHE. Furthermore, Zn_3Al_1 and Zn_4Al_1 LDHs showed a significant change relating to ZnO impurities in the XRD patterns and SEM images before and after the CO_2RR whereas Zn_2Al_1 LDH did not show it. These results indicate that Zn-Al LDH is promising as a CO_2RR electrocatalyst for CO formation.

ARTICLE HISTORY
Received 27 December 2022
Accepted 11 July 2023

KEYWORDS
CO_2 reduction; CO formation; electrocatalyst; layered double hydroxide

1. Introduction

In recent years, carbon dioxide (CO_2) reduction reactions (CO_2RR) have been attracting attention as a technology to achieve carbon neutrality, using surplus electricity generated from renewable energy sources such as solar and wind power [1,2]. Processes of CO_2RR include photochemical, biochemical, and electrochemical reduction [3]. Among these processes, the electrochemical reduction is expected to have higher productivity, higher energy conversion efficiency, and higher sustainability than the other processes because surplus electricity can be used directly as an energy source [4]. Furthermore, the products of CO_2RR include various reduction products such as carbon monoxide (CO), methane (CH_4), methanol (CH_3OH), formic acid (HCOOH), and C_2 products, and selectively obtaining products is also considered an important function. Among these, CO can be used as a raw material for various chemicals: for example, the Fischer-Tropsch method can be used to synthesize liquid hydrocarbon fuels. Equation (1)–(3) shows the reaction of electrochemical reduction of CO_2 to CO under alkaline conditions.

$$\text{Cathode}: CO_2 + H_2O + 2e^- \rightarrow CO + 2OH^- \quad E^o = -0.11\ \text{Vvs.RHE} \tag{1}$$

$$\text{Anode}: 2OH^- \rightarrow H_2O + 2e^- + (1/2)O_2 \quad E^o = +1.23\ \text{Vvs.RHE} \tag{2}$$

$$\text{Total reaction}: CO_2 \rightarrow CO + (1/2)O_2 \tag{3}$$

As shown in Equation (1), the formation of CO by CO_2 RR on the cathode side involves the formation of hydroxide ions (OH^-), and its activity tends to increase under alkaline conditions [5]. The CO_2RR electrocatalyst must have high durability against alkaline conditions. Current research on CO-forming CO_2RR has shown that catalysts using precious metals such as silver and gold have high catalytic efficiency [6]. However, precious metals are a limited resource, and there is a need to develop inexpensive electrocatalysts that do not use precious metals.

We focused on layered double hydroxide (LDH) as a material to solve this problem. LDH has the general composition $[M^{2+}_{1-x}M^{3+}_x(OH)_2]^{x+}$ $[A^{n-}_{x/n}{\cdot}yH_2O]^{x-}$ as shown in Figure 1, which is composed of positively charged metal hydroxide layers containing divalent and trivalent metal ions (M^{2+} and M^{3+})

CONTACT Nataly Carolina Rosero-Navarro rosero@eng.hokudai.ac.jp Faculty of Engineering, Hokkaido University, Kita-ku, Sapporo, Hokkaido 060-8628, Japan; Kiyoharu Tadanaga tadanaga@eng.hokudai.ac.jp

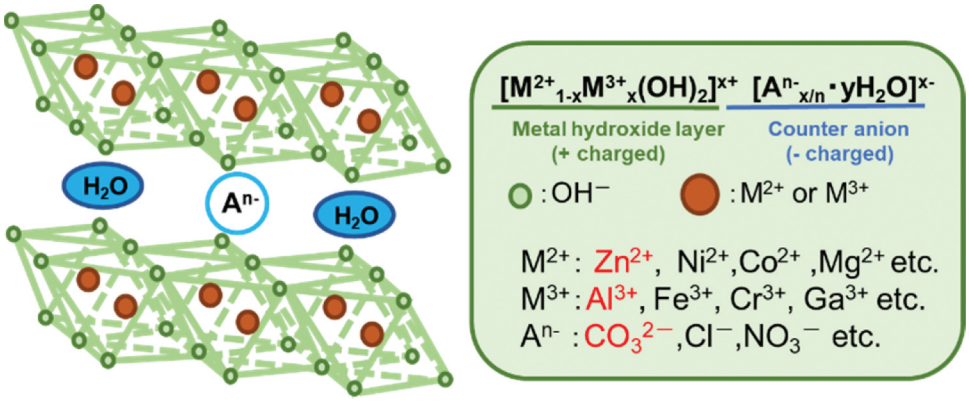

Figure 1. Structure of LDH ($[M^{2+}_{1-x}M^{3+}_{x}(OH)_2]^{x+}$ $[A^{n-}_{x/n}{\cdot}yH_2O]^{x-}$).

and charge compensating anions (A^{n-}) and water inserted between the layers. The advantages of using LDH as a catalyst include high stability in alkaline solutions [7], high hydroxide ion conductivity [8], various metal compositions [9], and large specific surface area [9]. These properties are also preferable to electrocatalysts for different reactions, and thus, transition metal-containing LDHs have been studied as electrocatalysts for oxygen evolution [7,10,11] and oxygen reduction reactions [7,10,12]. Recently, the application of Cu-Al LDHs as CO_2RR electrocatalysts has been reported, showing that Cu-Al-based LDHs can reduce CO_2 to CO and HCOOH [13]. Moreover, M-Al LDHs (M = Ni, Co) [14] and Zn-M LDHs (M = Al, Ti, Ga) [14,15] have also been reported to exhibit CO_2RR catalytic activity for "photocatalysis", and Zn-Al LDH was found to have the highest CO selectivity (90%) [15].

In this study, the electrocatalytic CO_2RR activity of Zn-Al LDHs was studied. Zn-Al LDHs loaded carbon sheets were prepared, and liquid-phase CO_2RR was performed to confirm the catalytic ability of Zn-Al LDH.

2. Experimental

2.1. Materials

Zinc nitrate hexahydrate ($Zn(NO_3)_2{\cdot}6\,H_2O$, 99.0%), aluminum nitrate nonahydrate ($Al(NO_3)_3{\cdot}9\,H_2O$, 98.0%), potassium bicarbonate ($KHCO_3$, > 99.5%), sodium carbonate (Na_2CO_3, 99.8%), and sodium hydroxide (NaOH, 97.0%) were purchased from FUJIFILM Wako Pure Chemical Co. Ethanol (EtOH, > 99.5%) was purchased from Kanto Chemical Co., Inc. Water was purified by a distilled water production system (SHIMIZU SCIENTIFIC INSTRUMENTS MFG Co., Ltd.). An anion exchange membrane (AHA) was purchased from Astom Corp. A CO_2 gas (>99.5%) was purchased from TAIYO NIPPON SANSO HOKKAIDO Corp. All the other solvents and chemicals in reagent grade were purchased and were used without further purification.

2.2. Preparation of Zn-Al LDHs

Zn-Al LDH intercalated with CO_3^{2-} (Zn-Al LDH) was prepared using the co-precipitation process [16]. $Zn(NO_3)_2{\cdot}6\,H_2O$ and $Al(NO_3)_3{\cdot}9\,H_2O$ were dissolved in deionized water with the molar ratio of Zn^{2+}/Al^{3+} = 2.0, 3.0, 4.0. The mixture was dropped into 0.30 M Na_2CO_3 solution with stirring at 80°C. The pH of the reaction mixture was adjusted to 10 by adding of 2.0 M aqueous NaOH solution with a pH meter (pH700, Eutech Instruments Pte. Ltd.). The obtained solution was aged at room temperature for 24 h. The resulting white precipitate was filtered, washed with distilled water, and dried at 50°C for 24 h.

The products were labeled Zn_2Al_1 LDH, Zn_3Al_1 LDH, and Zn_4Al_1 LDH, corresponding to the starting composition ratio of Zn and Al. The products were characterized by X-ray diffraction (XRD), scanning electron microscopy coupled with energy-dispersive X-ray spectrometry (SEM-EDX), field emission SEM (FE-SEM), and inductively coupled plasma atomic emission spectrometer (ICP-AES). To identify the crystalline phase, XRD patterns (CuKα) were taken using an XRD diffractometer (Mini Flex 600, Rigaku Corp.). The sample morphology and chemical composition were determined by SEM-EDX (TM3030, Hitachi Ltd.; SwiftED3000, Oxford Instruments), FE-SEM (JSM-7001FA, JEOL Ltd.), and ICP-AES (ICPE-9000, Shimadzu Corp.).

2.3. Preparation of the LDH-loaded carbon sheet as a working electrode

The LDH-loaded carbon sheet was prepared by the following procedure. First, 7.5 mg of the Zn-Al LDH, 7.5 mg of the conductive aid (Vulcan XC72, Cabot Corp.), and 6.0 µL of the binder (Teflon solution: 60 mass% ethylenechlorotrifluoroethylene copolymer (ECTFE)) were mixed by grinding, resulting in the film-

like mixture. The obtained mixture was pressed onto a carbon sheet at 3 MPa for 10 s and 5 MPa for 30 s, and the excess area of the mixture was cut. The coating area was 1.0 cm^2 with a 1.0 cm square shape.

2.4. Electrocatalytic CO_2RR experiment

Electrocatalytic CO_2RR was carried out by using a three-electrode setup composed of a two-chamber cell (H-type cell), as shown in Fig. S1. The cathodic compartment and anodic compartment were separated by a piece of the anion exchange membrane to avoid the unexpected influence of the oxidation reaction taking place on the counter electrode. The LDH-loaded carbon sheet, a platinum wire electrode (CE-100A, EC FRONTIER Co., Ltd.), and Ag/AgCl electrode (3.0 M NaCl, BAS Inc.) were used as working, counter, and reference electrodes, respectively. A CO_2-saturated 0.10 M aqueous $KHCO_3$ solutions (pH = 7.0) was used as a catholyte, and a not-saturated one was used as an anolyte. The pH of the electrolyte solution was measured with a pH meter (pH700, Eutech Instruments Pte. Ltd.). The CO_2 gas flowed with 10 mL min^{-1} flow rate and 0.10 MPa inlet pressure to the cathodic compartment, and the catholyte solution was stirred at 600 rpm with a PTFE stirring bar. Under the above conditions, CO_2 electrolysis for 30 min was performed by applying a voltage with an electrochemical analyzer (Sp-200, Biologic). Gas-phase products were detected by gas chromatography techniques (GC-2014, Shimadzu Corp.; carrier gas: nitrogen, flow rate: 10 ml min^{-1}, pressure: 53.2 kPa, vaporization chamber temperature: 120°C). For the detection of hydrogen (H_2), Molecular Sieve 5A (GL Sciences Inc.; column temperature: 50°C, injected sample volume: 1 mL) and a thermal conductivity detector (TCD, Shimadzu Corp.; detector temperature: 120°C) were used. For the detection of CO and gaseous hydrocarbons, PoraPak N (GL Sciences Inc.; column temperature: 50°C, injected sample volume: 1 mL) for a flame ionization detector (FID, Shimadzu Corp.; detector temperature: 120°C) was used.

Electrode potentials in the study were converted to the reversible hydrogen electrode (RHE) or the standard hydrogen electrode (SHE) according to the following equations: $E_{RHE} = E_{SHE} + 0.059 \times pH$, $E_{SHE} = E_{Ag/AgCl} + 0.222$. All the potentials and voltages in this work were evaluated without iR calibration. The Faradaic efficiency (*FE*) for CO and H_2 was calculated based on the equation (4) [17].

$$FE = \frac{2VprF}{IRT} \quad (4)$$

Where *V* was the volume concentration of CO or H_2 in the produced gas from the reaction cell. *I* (mA) was the average current during the reaction, and *r* was the CO_2 flow rate (m^3 s^{-1}) at ambient temperature and pressure. For the other constants in the formula, *p* was 1.013×10^5 Pa, *F* was 96,485 C mol^{-1}, *R* was 8.3145 J mol^{-1} K^{-1}, and *T* was 298 K.

3. Results and discussion

3.1. Characterization of Zn-Al LDHs

Figures 2 and 3 show the XRD patterns and SEM images of precipitates prepared in this study. As shown in Figure 2, the (003) and (006) plane peaks, characteristic of the layered structure, were observed. In Zn_2Al_1 LDH, all the peaks were assigned to the previously reported XRD pattern of Zn-Al LDH with carbonate (CO_3^{2-}) anions as interlayer anions (($Zn_{0.66}Al_{0.34}(OH)_2)(CO_3)_{0.17}(H_2O)_{0.7}$) [16], without other impurity peaks. On the other hand, in Zn_3Al_1 and Zn_4Al_1 LDH,

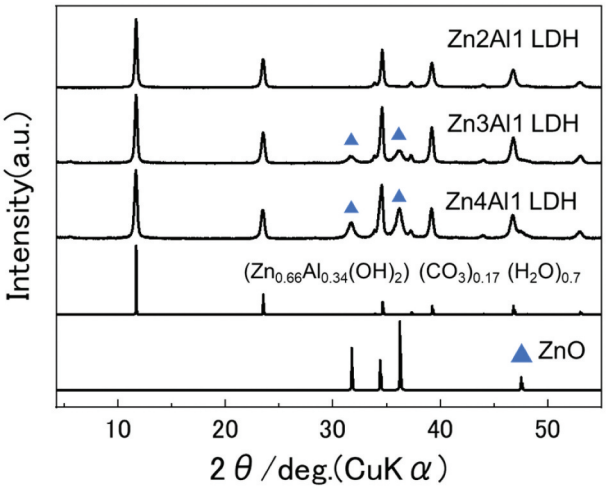

Figure 2. XRD patterns of Zn_2Al_1 (a), Zn_3Al_1 (b), and Zn_4Al_1 LDHs (c). The data of $(Zn_{0.66}Al_{0.34}(OH)_2)(CO_3)_{0.17}(H_2O)_{0.7}$ and ZnO were referred to [Reference 16 and 18], respectively.

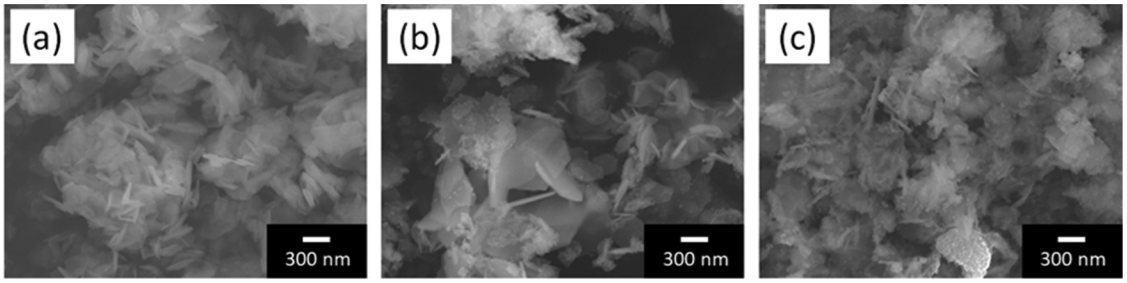

Figure 3. FE-SEM images of Zn_2Al_1 (a), Zn_3Al_1 (b), and Zn_4Al_1 LDHs (c).

the peaks of zinc oxide (ZnO) were observed as impurity peaks [18].

From the FE-SEM images, as shown in Figure 3, plate-like crystals, characteristic of LDH, with a size of 0.1–1 μm were observed in all the systems, but nanometer-order fine particles were also observed in Zn_3Al_1 and Zn_4Al_1 LDHs, which appeared to be the most abundant in Zn_4Al_1 LDH. These fine particles could be assigned to be ZnO, considering the XRD results. The SEM-EDX mapping showed that Zn^{2+} and Al^{3+} were homogeneously distributed on the particles in the micrometer-order in Zn_2Al_1 and Zn_3Al_1 LDH as shown in Figures S2 (a) and (b). On the other hand, a localized presence of Zn was observed in Zn_4Al_1 LDH as shown in the green circle of Figure S2 (c). This also indicates the presence of ZnO, considering the XRD results. The elemental analysis by ICP-AES showed the chemical composition with Zn^{2+}/Al^{3+} molar ratios of 2.16, 3.11, and 4.17 for Zn_2Al_1, Zn_3Al_1 and Zn_4Al_1 LDH, respectively. These ratios are almost the same as the starting composition ones.

These results are accordance with the previous studies with the urea method [19], as well as co-precipitation method [20,21]. One of them postulated that the crystallization of a hydrotalcite with a Zn^{2+}/Al^{3+} molar ratio of 2:1 occurred more preferentially rather than that of 3:1 [21]. Therefore, in the present study, it was considered that a hydrotalcite with a Zn^{2+}/Al^{3+} molar ratio of 2:1 was a main product even in Zn_3Al_1 and Zn_4Al_1 LDH systems, where excess Zn^{2+} ions were not incorporated into the hydroxide layer and were precipitated as ZnO.

3.2. Electrocatalytic CO_2RR experiment with LDH-loaded carbon sheet in 0.1 M aqueous $KHCO_3$ solution

In the electrocatalytic CO_2RR with Zn-Al LDHs, 0.1 M aqueous $KHCO_3$ solution was used as a typical electrolyte. The applied potential dependence of current density (*j*) and Faradaic efficiency (*FE*) are shown in Figures 4 and 5, respectively. As shown in Figure 4, the current density increased with more negative

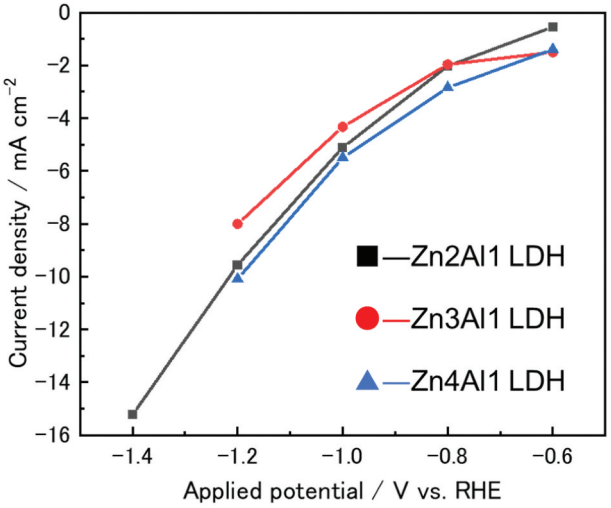

Figure 4. Applied potential dependence of current density (*j*) for electrocatalytic CO_2RR in 0.1 M aqueous $KHCO_3$ solution using each cathode with Zn_2Al_1 (black), Zn_3Al_1 (red), and Zn_4Al_1 LDHs (blue).

applied potentials in all the samples, and catalytic currents were observed. The total current densities in all the systems are almost the same at – 0.6 to –1.2 V vs. RHE. The additional measurement at –1.4 V vs. RHE was performed only for Zn_2Al_1 LDH, showing the maximum current density of –15.2 mA cm^{-2} at –1.4 V vs RHE. CO was observed as a major product and increased at more negative applied potentials in all the systems. For Zn_2Al_1 LDH, as shown in Figure 5 (a), the *FE* for CO (FE_{CO}) was 1, 18, 38, 63, and 77% at – 0.6, –0.8, –1.0, –1.2, and –1.4 V vs. RHE, respectively. And then, the hydrogen (H_2) formation was observed as a major side-reaction with the *FE* of 17–41%, and electron consumption by other reactions gave the *FE* of 6–41%. CH_4 was detected as a minor product but its *FE* was less than 0.5% for all the cathodes. In summary, the partial current density for CO formation (j_{CO}) of 11.7 mA cm^{-2} was obtained with 77% selectivity for CO and 94% selectivity for (CO + H_2) at –1.4 V vs. RHE for Zn_2Al_1 LDH. The highest FE_{CO} of 77% for Zn_2Al_1 LDH is lower than that of Au nanoparticles (the highest FE_{CO} of 97% [22]) reported so far, but higher than that of Cu-Al LDH (the highest FE_{CO} of 42% [13]) reported

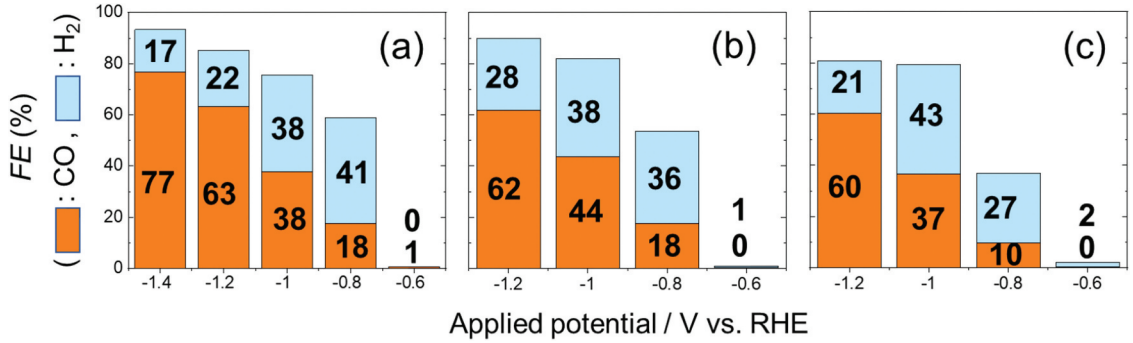

Figure 5. Applied potential dependence of Faradaic efficiency (*FE*) for electrocatalytic CO_2RR in 0.1 M aqueous $KHCO_3$ solution using each cathode with Zn_2Al_1 (a), Zn_3Al_1 (b) and Zn_4Al_1 LDHs (c). (orange bar: CO, blue bar: H_2).

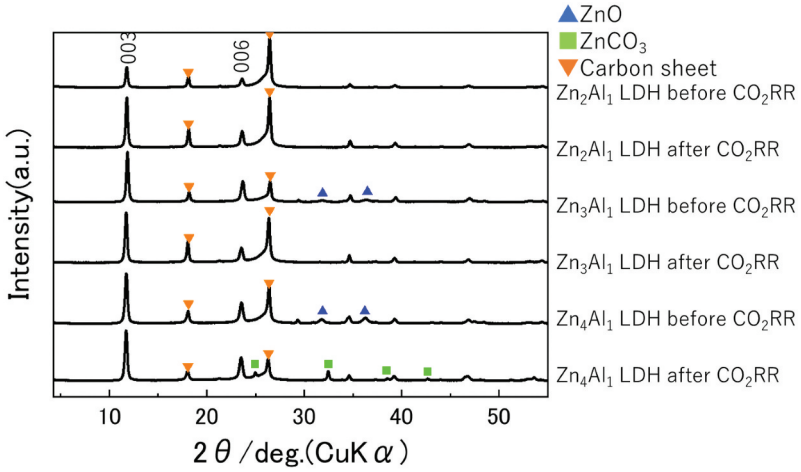

Figure 6. XRD patterns of Zn_2Al_1, Zn_3Al_1, and Zn_4Al_1 LDHs before and after the electrocatalytic CO_2RR experiment. The attribution of peaks for ZnO and $ZnCO_3$ was referred to [Reference 18 and 25], respectively.

previously, indicating that Zn_2Al_1 LDH is promising as a non-precious CO_2RR electrocatalyst for CO formation. For Zn_3Al_1 and Zn_4Al_1 LDHs, the *FE* of each product did not differ significantly to Zn_2Al_1 LDH at all the applied potentials, suggesting that all of them acted as CO_2RR electrocatalysts and ZnO in Zn_3Al_1 and Zn_4Al_1 LDHs did not have a significant contribution to CO formation. Zn is known to be the only earth-abundant monometallic electrocatalyst with high CO selectivity, but bulk Zn catalysts tend to show large overpotentials and slow reaction rates due to small numbers of active sites [23]. Since the monovalent Zn^+ ($3d^{10}4s^1$) site has been found to be an active site in many cases due to its coordinatively unsaturated characteristics [24], the monovalent Zn^+ site could also act as an active site in the case of Zn-Al LDHs.

Figure 6 shows the XRD patterns of Zn_2Al_1, Zn_3Al_1, Zn_4Al_1 LDHs before and after CO_2RR. In all the systems, the Zn-Al LDH peaks were observed even after CO_2RR, where the peak positions did not change. On the other hand, the ZnO peaks disappeared in Zn_3Al_1 and Zn_4Al_1 LDHs, and new peaks corresponding to zinc carbonate ($ZnCO_3$) [25] appeared in Zn_4Al_1 LDH, while no peaks other than Zn-Al LDH was observed in Zn_2Al_1 LDH after CO_2RR.

Figure S3 shows the SEM images of the carbon sheet loaded with Zn-Al LDHs before and after CO_2 RR. In all the LDHs, significant changes in the size of particles were not observed at the major region. However, only in Zn_4Al_1 LDH, new spherical particles of about 1 µm were locally observed after CO_2RR as shown in Figure S4(d). These spherical particles were indicated to be $ZnCO_3$ derived from dissolved ZnO considering the XRD results. This is also supported by the EDX mappings as shown in Figure S4, where the local region occupied by the spherical particles clearly showed more zinc components than the major region. The above XRD and SEM-EDX results suggest that Zn-Al LDH is electrochemically more stable than ZnO under the present experimental conditions.

4. Conclusion

Electrocatalytic activity for CO_2RR of Zn-Al LDH was studied using Zn-Al LDH embedded carbon sheet. Zn-Al LDH exhibited the CO_2RR electrocatalytic activity for CO formation in CO_2RR in an aqueous $KHCO_3$ solution. With Zn_2Al_1 LDH as an electrocatalyst, the current density of $-15.2\,mA\,cm^{-2}$ was obtained with 77% selectivity for CO and 94% selectivity for $(CO + H_2)$ at $-1.4\,V$ vs. RHE. Zn_2Al_1 LDH before and after constant potential electrolysis, there is no significant change in structure. These results show that Zn_2Al_1 LDH is promising as a CO_2RR electrocatalyst for CO formation.

Acknowledgments

This research was supported through 4AirCRAFT project under the strategic international cooperation between European Union (Horizon 2020, No.101022633) and Japan Science and Technology Agency (JST) with reference number JPMJSC2102.

Disclosure statement

No potential conflict of interest was reported by the author(s).

Funding

The work was supported by the Japan Science and Technology Agency [JPMJSC2102]; European Union's Horizon 2020 research and innovation programme [101022633].

ORCID

Ryosuke Nakazato http://orcid.org/0009-0008-8544-8053
Nataly Carolina Rosero-Navarro http://orcid.org/0000-0001-6838-2875
Akira Miura http://orcid.org/0000-0003-0388-9696
Kiyoharu Tadanaga http://orcid.org/0000-0002-3319-4353

References

[1] Tatin A, Bonin J, Robert M. A case for electrofuels. ACS Energy Lett. 2016;1(5):1062–1064. doi: 10.1021/acsenergylett.6b00510

[2] De LP, Hahn C, Higgins D, et al. What would it take for renewably powered electrosynthesis to displace petrochemical processes? Science. 2019;364(6438): eaav3506. doi: 10.1126/science.aav3506

[3] Qiao J, Liu Y, Hong F, et al. A review of catalysts for the electroreduction of carbon dioxide to produce low-carbon fuels. Chem Soc Rev. 2014;43(2):631–675. doi: 10.1039/C3CS60323G

[4] Kamiya K, Fujii K, Sugiyama M, et al. CO_2 electrolysis in integrated artificial photosynthesis systems. Chem Lett. 2021;50(1):166–179. doi: 10.1246/cl.200691

[5] Luo W, Zhang Q, Zhang J, et al. Electrochemical reconstruction of ZnO for selective reduction of CO2 to CO. Appl Catal B Environ. 2020;273(15):119060. Elsevier B. V. doi: 10.1016/j.apcatb.2020.119060

[6] Cheng W-H, Richter MH, Sullivan I, et al. CO_2 reduction to CO with 19% efficiency in a solar-driven gas diffusion electrode flow cell under outdoor solar illumination. ACS Energy Lett American Chem Soc. 2020;5(2):470–476. doi: 10.1021/acsenergylett.9b02576

[7] Kowsari H, Mehrpooya M, Pourfayaz F. Nitrogen and sulfur doped ZnAl layered double hydroxide/reduced graphene oxide as an efficient nanoelectrocatalyst for oxygen reduction reactions. Int J Hydrogen Energy. 2020;45(51): 27129–27144. Elsevier Ltd.

[8] Tadanaga K, Furukawa Y, Hayashi A, et al. Direct ethanol fuel cell using hydrotalcite clay as a hydroxide ion conductive electrolyte. Adv Mater. 2010;22 (39):4401–4404. doi: 10.1002/adma.201001766

[9] Ezeh CI, Tomatis M, Yang X, et al. Ultrasonic and hydrothermal mediated synthesis routes for functionalized Mg-Al LDH: Comparison study on surface morphology, basic site strength, cyclic sorption efficiency and effectiveness. Ultrason Sonochem. 2018;40:341–352. Elsevier B.V. doi: 10.1016/j.ultsonch.2017.07.013

[10] Lu L, Zheng Y, Yang R, et al. Recent advances of layered double hydroxides–based bifunctional electrocatalysts for ORR and OER. Mater Today Chem. 2021;21:100488. doi:10.1016/j.mtchem.2021.100488. Elsevier Ltd.

[11] Arishige Y, Kubo D, Tadanaga K, et al. Electrochemical oxygen separation using hydroxide ion conductive layered double hydroxides. Solid State Ion. 2014;262:238–240. Elsevier. doi: 10.1016/j.ssi.2013.09.009

[12] Iwai Y, Miura A, Rosero-Navarro NC, et al. Composition, valence and oxygen reduction reaction activity of Mn-based layered double hydroxides. J Asian Ceram Soc. 2019;7(2):147–153. doi:10.1080/21870764.2019.1581321. Taylor and Francis Ltd.

[13] Iwase K, Hirano T, Honma I. Copper aluminum layered double hydroxides with different compositions and morphologies as electrocatalysts for the carbon dioxide reduction reaction. ChemSuschem. 2022;15(2): e202102340. doi:10.1002/cssc.202102340. John Wiley and Sons Inc.

[14] Bai S, Wang Z, Tan L, et al. 600 nm irradiation-induced efficient photocatalytic CO_2 reduction by ultrathin layered double hydroxide nanosheets. Ind Eng Chem Res American Chem Soc. 2020;59(13):5848–5857. doi: 10.1021/acs.iecr.0c00522

[15] Xiong X, Zhao Y, Shi R, et al. Selective photocatalytic CO_2 reduction over Zn-based layered double hydroxides containing tri or tetravalent metals. Sci Bull. 2020;65(12):987–994. Elsevier B.V. doi: 10.1016/j.scib.2020.03.032

[16] Yasaei M, Khakbiz M, Zamanian A, et al. Synthesis and characterization of Zn/Al-LDH@SiO_2 nanohybrid: Intercalation and release behavior of vitamin C. Mater Sci Eng C. 2019;103:109816. doi:10.1016/j.msec.2019.109816. Elsevier Ltd.

[17] Wu X, Sun JW, Liu PF, et al. Molecularly dispersed cobalt phthalocyanine mediates selective and durable CO_2 reduction in a membrane flow cell. Adv Funct Mater. 2022;32(11):2107301. doi:10.1002/adfm.202107301.

[18] Zak AK, Abrishami M, Majid, WHA, et al. Effects of annealing temperature on some structural and optical properties of ZnO nanoparticles prepared by a modified sol–gel combustion method. Ceram. Int. 2011;37 (1):393–398. doi: 10.1016/j.ceramint.2010.08.017

[19] Liu Z, Ma R, Ebina Y, et al. General synthesis and delamination of highly crystalline transition-metal-bearing layered double hydroxides. Langmuir. 2007;23(2):861–867. doi: 10.1021/la062345m

[20] Xu Z, Shi J, Haroone MS, et al. Zinc-aluminum oxide solid solution nanosheets obtained by pyrolysis of layered double hydroxide as the photoanodes for dye-sensitized solar cells. J Colloid Interface Sci. 2018;515:240–247. Elsevier Inc. doi: 10.1016/j.jcis.2018.01.037

[21] Kloprogge JT, Hickey L, Frost RL. The effects of synthesis pH and hydrothermal treatment on the formation of zinc aluminum hydrotalcites. J Solid State Chem. 2004;177(11):4047–4057. doi: 10.1016/j.jssc.2004.07.010

[22] Zhu W, Michalsky R, Metin Ö, et al. Monodisperse Au nanoparticles for selective electrocatalytic reduction of CO_2 to CO. J Am Chem Soc. 2013;135 (45):16833–16836. doi: 10.1021/ja409445p

[23] Hori Y, Wakebe H, Tsukamoto T, et al. Electrocatalytic process of CO selectivity in electrochemical reduction of CO_2 at metal electrodes in aqueous media. Electrochim Acta. 1994;39(11–12):1833–1839. doi: 10.1016/0013-4686(94)85172-7

[24] Chen G, Zhao Y, Shang L, et al. Recent advances in the synthesis, characterization and application of Zn + -containing heterogeneous catalysts. Adv Sci. 2016;3 (7):1500424. doi: 10.1002/advs.201500424

[25] Liang W, Bai J, Li Z, et al. Crystal growth, structure and thermal properties of anhydrous zinc carbonate ($ZnCO_3$). J Alloys Compd. 2022;898:162916. Elsevier. doi: 10.1016/j.jallcom.2021.162916